

# A NonLinear Observer of an Electrical Transformer: A Bond Graph Approach

Gilberto Gonzalez-A , Israel Nuñez

**Abstract**—A bond graph model of an electrical transformer including the nonlinear saturation is presented. A nonlinear observer for the transformer based on multivariable circle criterion in the physical domain is proposed. In order to show the saturation and hysteresis effects on the electrical transformer, simulation results are obtained. Finally, the paper describes that convergence of the estimates to the true states is achieved.

**Keywords**— Bond graph, nonlinear observer, electrical transformer, nonlinear saturation.

## I. INTRODUCTION

TRANSFORMERS make large power systems possible. To transmit hundreds of megawatts of power efficiently over long distances. The main uses of electrical transformers are for changing the magnitude of an AC voltage providing electrical isolation, and matching the load impedance to the source [1].

On the other hand, a bond graph is a model of a dynamic system where a collection of components interact with each other through energy ports. A bond graph consist of subsystems linked by lines to show the energetic connections. It can represent a variety of energy types and can describe how the power flows through the system [2], [3].

Also, the principle of observability intuitively establishes the possibility to rebuilt the state variables from the measured outputs and given inputs. With observability conditions, the observation problem consists in seeking a state estimation by means of an auxiliary dynamic system, the observer [4].

Some papers have been published applying bond graph to construct an observer. In [5] proposes a control in bond graph using state estimated feedback for MIMO LTI systems. In [6] a bond graph approach to built reduced order observers for LTI systems is described. This approach uses the bicausality concept to simplify the construction and the calculation of the observer. A bond graph representation of model-based control, which allows the design of controllers in the physical domain is described in [7].

In other wise many papers have been published on observers, for example [8] gives an approach to estimate the state of a nonlinear system from the point of view of differential algebra. However, in [9] and [10] globally convergent observers are designed for a class of systems with multivariable nonlinearities.

According with transformers, in [11] a magnetic circuit model of power transformer which takes into account the nonlinear hysteresis phenomenon is analyzed. However, this paper uses a special nonlinear function to introduce the hysteresis. In [13] a bond graph model of a transformer based on a nonlinear

conductive magnetic circuit is described. Here, the state space nonlinear magnetic model has to be known.

Therefore, in this paper a bond graph model of a transformer with two windings is proposed. Also, a basic electromagnetic model for the magnetizing branch of a transformer with two or three windings in the physical domain is described. This magnetizing branch consists of a resistor and inductance. However, in order to introduce the magnetic saturation a nonlinear function is used.

The outline of the paper is as follows: Section II gives some basic elements of the modelling in bond graph. Section III summarizes the model of a two winding transformer including the flux linkage and voltage equations. Section IV describes the observers design for a class of nonlinear system with multivariable nonlinearities. A bond graph model of a transformer with two windings considering the nonlinear core is proposed in section V. A nonlinear observer in the physical domain is presented in section VI. A bond graph of the complete system formed by the transformer and the observer is proposed in section VII. Finally, section VIII gives the conclusions.

## II. MODELLING IN BOND GRAPH

The bond graph methodology allows to model a system in a simple and direct manner. Using fields and junction structures, one may conveniently study systems containing complex multiport components using bond graphs. In fact, bond graphs with fields prove to be a most effective way to handle the modeling of complex multiport systems [2].

Consider the following scheme of a multiport LTI system which includes the key vectors of Fig. 1 [2], [14].

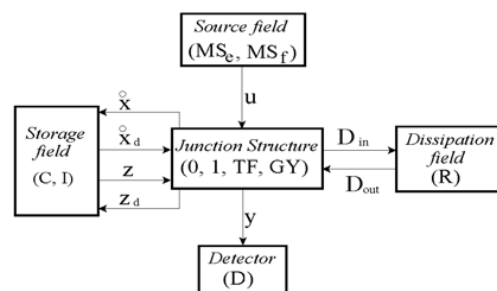


Fig. 1. Key vectors of a bond graph.

In Fig. 1,  $(MS_e, MS_f)$ ,  $(C, I)$ ,  $(R)$  and  $(D)$  denote the source, the energy storage, the energy dissipation and the detector fields, and  $(0, 1, TF, GY)$  the junction structure with transformers,  $TF$ , and gyrators,  $GY$ .

The state  $x \in \mathcal{R}^n$  and  $x_d \in \mathcal{R}^m$  are composed of energy variables  $p$  and  $q$  associated with  $I$  and  $C$  elements in integral and derivative causality, respectively,  $u \in \mathcal{R}^p$  denotes the plant

input,  $y \in \mathbb{R}^q$ , the plant output,  $z \in \mathbb{R}^n$  the co-energy vector,  $z_d \in \mathbb{R}^m$  the derivative co-energy and  $D_{in} \in \mathbb{R}^r$  and  $D_{out} \in \mathbb{R}^r$  are a mixture of  $e$  and  $f$  showing the energy exchanges between the dissipation field and the junction structure.

The relations of the storage and dissipation field are,

$$z = Fx \quad (1)$$

$$z_d = F_d x \quad (2)$$

$$D_{out} = LD_{in} \quad (3)$$

The relations of the junction structure are [2], [14],

$$\begin{bmatrix} \dot{x} \\ D_{in} \\ y \end{bmatrix} = \begin{bmatrix} S_{11} & S_{12} & S_{13} & S_{14} \\ S_{21} & S_{22} & S_{23} & 0 \\ S_{31} & S_{32} & S_{33} & 0 \end{bmatrix} \begin{bmatrix} z \\ D_{out} \\ u \\ \dot{x}_d \end{bmatrix} \quad (4)$$

$$z_d = -S_{14}^T z$$

The entries of  $S$  take values inside the set  $\{0, \pm 1, \pm K_m, \pm K_n\}$  where  $K_m$  and  $K_n$  are transformer and gyrator modules;  $S_{11}$  and  $S_{22}$  are square skew-symmetric matrices and  $S_{12}$  and  $S_{21}$  are matrices each other negative transpose. The state equation is,

$$\dot{x} = A_p x + B_p u \quad (5)$$

$$y = C_p x + D_p u \quad (6)$$

where

$$A_p = E^{-1} (S_{11} + S_{12} M S_{21}) F \quad (7)$$

$$B_p = E^{-1} (S_{13} + S_{12} M S_{23}) \quad (8)$$

$$C_p = (S_{31} + S_{32} M S_{21}) F \quad (9)$$

$$D_p = S_{33} + S_{32} M S_{23} \quad (10)$$

being

$$E = I_n + S_{14} F_d^{-1} S_{14}^T F \quad (11)$$

$$M = (I_n - L S_{22})^{-1} L \quad (12)$$

It is very common in electrical power systems to use the electrical current as state variable of this manner taking the derivative of (1) and (5), we have

$$\dot{z} = \overline{A}_p z + \overline{B}_p u \quad (13)$$

$$y = \overline{C}_p z + D_p u \quad (14)$$

where

$$\overline{A}_p = F A_p F^{-1} \quad (15)$$

$$\overline{B}_p = F B_p \quad (16)$$

$$\overline{C}_p = C_p F^{-1} \quad (17)$$

Next section summarizes the basic elements of an electrical transformer.

### III. MODEL OF A TWO-WINDING TRANSFORMER

Charles P. Steinmetz (1865-1923) developed the circuit model that is universally used for the analysis of iron core transformers at power frequencies. His model has many advantages over those resulting from straightforward application of linear circuit theory, primarily because the iron core exhibits

saturation and hysteresis and is thus definitely nonlinear [1]. However it is good idea to consider transformers first from the point of view of basic linear circuit theory to better appreciate the Steinmetz model.

#### A. Flux Linkage Equations

Consider the magnetic coupling between the primary and secondary windings of a transformer shown in Fig. 2 [12].

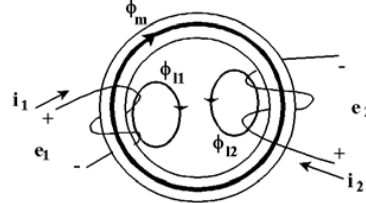


Fig. 2. Magnetic coupling of a two-winding transformer.

The total flux linked by each winding may be divided into two components: a mutual component,  $\phi_m$ , that is common to both windings, and a leakage flux components that links only the winding itself. In terms of these flux components, the total flux by each of the windings can be expressed as,

$$\phi_1 = \phi_{l1} + \phi_m \quad (18)$$

$$\phi_2 = \phi_{l2} + \phi_m \quad (19)$$

where  $\phi_{l1}$  and  $\phi_{l2}$  are the leakage flux components of windings 1 and 2, respectively. Assuming that  $N_1$  turns of winding 1 effectively link  $\phi_m$  and  $\phi_{l1}$ , the flux linkage of winding 1 is defined by,

$$\lambda_1 = N_1 \phi_1 = N_1 (\phi_{l1} + \phi_m) \quad (20)$$

the leakage and mutual fluxes can be expressed in terms of the winding currents using the magneto-motive forces (mmfs) and permeances. So, the flux linkage of winding 1 is,

$$\lambda_1 = N_1 [N_1 i_1 P_{l1} + (N_1 i_1 + N_2 i_2) P_m] \quad (21)$$

where  $P_{l1} = \frac{\phi_{l1}}{N_1 i_1}$  and  $P_m = \frac{\phi_m}{N_1 i_1 + N_2 i_2}$ .

Similarly, the flux linkage of winding 2 can be expressed as,

$$\lambda_2 = N_2 (\phi_{l2} + \phi_m) \quad (22)$$

and using mmfs and permeances for this winding,

$$\lambda_2 = N_2 [N_2 i_2 P_{l2} + (N_1 i_1 + N_2 i_2) P_m] \quad (23)$$

The resulting flux linkage equations for the two magnetically coupled windings, expressed in terms of the winding inductances are,

$$\begin{bmatrix} \lambda_1 \\ \lambda_2 \end{bmatrix} = \begin{bmatrix} L_{11} & L_{12} \\ L_{21} & L_{22} \end{bmatrix} \begin{bmatrix} i_1 \\ i_2 \end{bmatrix} \quad (24)$$

where  $L_{11}$  and  $L_{22}$  are the self-inductances of the windings, and  $L_{12}$  and  $L_{21}$  are the mutual inductances between them.

Note that the self-inductance of the primary can be divided into two components, the primary leakage inductance,  $L_{l1}$  and the primary magnetizing inductance,  $L_{m1}$ , which are defined by,

$$L_{11} = L_{l1} + L_{m1} \quad (25)$$

where  $L_{l1} = N_1^2 P_{l1}$  and  $L_{m1} = N_1^2 i_1 P_m$ .

Likewise, for winding 2

$$L_{22} = L_{l2} + L_{m2} \tag{26}$$

where  $L_{l2} = N_2^2 P_{l2}$  and  $L_{m2} = N_2^2 i_2 P_m$ .

Finally, the mutual inductance is given by,

$$L_{12} = N_1 N_2 i_2 P_m \tag{27}$$

$$L_{21} = N_1 N_2 i_1 P_m \tag{28}$$

Taking the ratio of  $L_{m2}$  a  $L_{m1}$ ,

$$L_{m2} = \frac{N_2 \phi_m}{i_2} = \frac{N_2 L_{12}}{N_1} = N_2^2 P_m = \left(\frac{N_2}{N_1}\right)^2 L_{m1} \tag{29}$$

### B. Voltage Equations

The induced voltage in winding 1 is given by,

$$e_1 = \frac{d\lambda_1}{dt} = L_{l1} \frac{di_1}{dt} + L_{12} \frac{di_2}{dt} \tag{30}$$

replacing  $L_{l1}$  by  $L_{l1} + L_{m1}$  and  $L_{12}i_2$  by  $N_2 L_{m1} i_2 / N_1$ , we obtain

$$e_1 = L_{l1} \frac{di_1}{dt} + L_{m1} \frac{d(i_1 + (N_2/N_1) i_2)}{dt} \tag{31}$$

Similarly, the induced voltage of winding 2 is written by,

$$e_2 = L_{l2} \frac{di_2}{dt} + L_{m2} \frac{d(i_2 + (N_1/N_2) i_1)}{dt} \tag{32}$$

Finally, the terminal voltage of a winding is the sum of the induced voltage and the resistive drop in the winding, the complete equations of the two windings are,

$$\begin{bmatrix} v_1 \\ v_2 \end{bmatrix} = \begin{bmatrix} r_1 i_1 \\ r_2 i_2 \end{bmatrix} + \begin{bmatrix} L_{l1} + L_{m1} & a^{-1} L_{m1} \\ a L_{m2} & L_{l2} + L_{m2} \end{bmatrix} \begin{bmatrix} \frac{di_1}{dt} \\ \frac{di_2}{dt} \end{bmatrix} \tag{33}$$

where  $a = N_1/N_2$ .

Next section describes the design of an observer for systems with multivariable monotone nonlinearities.

## IV. NONLINEAR OBSERVER

This section describes a nonlinear observer design with multivariable nonlinearities. This design represents the observer error system as the feedback interconnection of a linear system and a state-dependent sector nonlinearity [9].

Firstly, this observer uses the multivariable nonlinearities  $\gamma(\cdot) : \mathbb{R}^l \rightarrow \mathbb{R}^l$  which satisfy a multivariable analog of the monotonicity property:

$$\frac{\partial \gamma}{\partial v} + \left(\frac{\partial \gamma}{\partial v}\right)^T \geq 0 \quad \forall v \in \mathbb{R}^l \tag{34}$$

With this property, the state nonlinearity that arises in the observer error system a multivariable sector condition

For our observer design, we consider the plant

$$\begin{aligned} \dot{x} &= Ax + G\gamma(Hx) + Bu \\ y &= Cx \end{aligned} \tag{35}$$

where  $x \in \mathbb{R}^n$  is the state,  $y \in \mathbb{R}^q$  is the measured output,  $u \in \mathbb{R}^p$  is the control input, and the multivariable nonlinearity  $\gamma(\cdot) : \mathbb{R}^l \rightarrow \mathbb{R}^l$  satisfies (34).

With this assumption, our observer has the same form as in [16]:

$$\dot{\hat{x}} = A\hat{x} + L(C\hat{x} - y) + G\gamma(H\hat{x} + K(C\hat{x} - y)) + Bu \tag{36}$$

Our task is to determine the observer matrices  $K \in \mathbb{R}^{l \times q}$  and  $L \in \mathbb{R}^{n \times q}$  to make the observer error  $e = x - \hat{x}$  approach zero. From (35) and (36), the dynamics of the observer error  $e = x - \hat{x}$  are governed by

$$\dot{e} = (A + LC)e + G[\gamma(v) - \gamma(w)], \tag{37}$$

where

$$v = Hx, \quad w = H\hat{x} + K(C\hat{x} - y) \tag{38}$$

We begin the observer design by representing the observer error system (37) as the feedback interconnection of a linear system and multivariable sector nonlinearity. To this end, we view  $\gamma(v) - \gamma(w)$  as a function of  $v$  and  $z = v - w = (H + KC)e$ ; that is, a state-dependent multivariable nonlinearity in  $z$ :

$$\varphi(v, z) = \gamma(v) - \gamma(w) \tag{39}$$

Substituting (39), we rewrite the observer error system (37) as

$$\begin{aligned} \dot{e} &= (A + LC)e + G\varphi(v, z) \\ z &= (H + KC)e \end{aligned} \tag{40}$$

To show that  $\varphi(v, z)$  satisfies a multivariable sector property, we make use the Mean Value Theorem [9], and rewrite  $\varphi(v, z)$  as

$$\begin{aligned} \varphi(v, z) &= \gamma(v) - \gamma(w) \\ &= \int_0^1 \left[ \frac{\partial \gamma}{\partial s} \right]_{s=v+\lambda(w-v)} (v - w) d\lambda \\ &= \int_0^1 \left[ \frac{\partial \gamma}{\partial s} \right]_{s=v-\lambda z} z d\lambda \end{aligned} \tag{41}$$

Thus, from property (34),

$$z^T \varphi(v, z) = \frac{1}{2} z^T \int_0^1 \left( \left[ \frac{\partial \gamma}{\partial s} \right] + \left[ \frac{\partial \gamma}{\partial s} \right]^T \right)_{s=v-\lambda z} d\lambda z \geq 0 \tag{42}$$

Thanks to this sector property, asymptotic stability is guaranteed from the circle criterion if the linear system with input  $\vartheta = -\varphi(v, z)$  and output  $z$  is SPR, that is, if a matrix  $P = P^T > 0$ , and a constant  $\varsigma > 0$  can be found such that [9]

$$\begin{bmatrix} (A + LC)^T P + P(A + LC) + \varsigma I & PG + (H + KC)^T \\ G^T P + (H + KC) & 0 \end{bmatrix} \leq 0 \tag{43}$$

Thus, the observer design for system (35) consists on solving (43), which is LMI in  $P = P^T \geq 0$ ,  $P, L, K$  and  $\varsigma \geq 0$ .

Next section proposes a two windings transformer including the linear and nonlinear core in the physical domain.

### V. BOND GRAPH OF A TWO WINDINGS TRANSFORMER WITH CORE

The final concept involved in the Steinmetz transformer model is a scheme for handling the nonlinearity of the core and the core losses. The Steinmetz model approaches the problem of representing core excitation by first dividing it into two parts: magnetization and core losses [1]. In order to consider the core losses of a transformer a bond graph model is presented in Fig. 3.

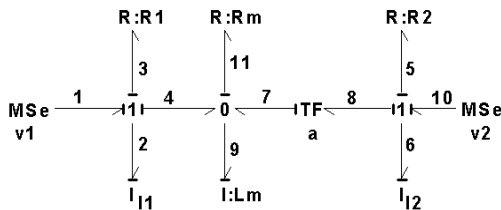


Fig. 3. Bond graph of a complete transformer.

The key vectors of the bond graph of Fig. 3 are,

$$x = \begin{bmatrix} p_2 \\ p_6 \\ p_9 \end{bmatrix}; \dot{x} = \begin{bmatrix} e_2 \\ e_6 \\ e_9 \end{bmatrix}; z = \begin{bmatrix} f_2 \\ f_6 \\ f_9 \end{bmatrix} \quad (44)$$

$$D_{in} = \begin{bmatrix} f_3 \\ f_5 \\ f_{11} \end{bmatrix}; D_{out} = \begin{bmatrix} e_3 \\ e_5 \\ e_{11} \end{bmatrix}; u = \begin{bmatrix} e_1 \\ e_{10} \end{bmatrix}$$

the constitutive relations of the fields are,

$$L = \text{diag}\{R_1, R_2, R_m\} \quad (45)$$

$$F = \text{diag}\left\{\frac{1}{L_{l1}}, \frac{1}{L_{l2}}, \frac{1}{L_m}\right\} \quad (46)$$

and the junction structure is given by

$$S_{12} = -S_{12}^T = \begin{bmatrix} -1 & 0 & -1 \\ 0 & -1 & \frac{-1}{a} \\ 0 & 0 & 1 \end{bmatrix}; S_{13} = \begin{bmatrix} 1 & 0 \\ 0 & 1 \\ 0 & 0 \end{bmatrix} \\ S_{11} = S_{22} = S_{23} = 0 \quad (47)$$

By substituting (45), (46) and (47) into (7) and 8, the state space representation of the transformer is,

$$\overline{A}_p = \begin{bmatrix} \frac{-(R_1+R_m)}{L_{l1}} & \frac{-R_m}{aL_{l1}} & \frac{R_m}{L_{l1}} \\ \frac{-R_m}{aL_{l2}} & \frac{-(R_1+R_m/a^2)}{L_{l1}} & \frac{-R_m}{aL_{l2}} \\ \frac{R_m}{L_m} & \frac{-R_m}{aL_m} & \frac{-R_m}{L_m} \end{bmatrix} \\ \overline{B}_p = \begin{bmatrix} \frac{1}{L_{l1}} & 0 & 0 \\ 0 & \frac{1}{L_{l2}} & 0 \end{bmatrix}^T \quad (48)$$

The incorporation of nonlinear effects such as magnetic saturation and hysteresis is achieved in the transformer model with the appropriate modification of the inductance  $L_m$  in the bond graph of Fig. 8.

In Fig. 4 the saturation curve is illustrated and this curve is approximated with the equation [15],

$$i_{L_m} = \frac{1}{\beta} \tan\left(\frac{\lambda L_m}{\alpha}\right) \quad (49)$$

where  $\alpha = 0.3215$  and  $\beta = 0.8642$ .

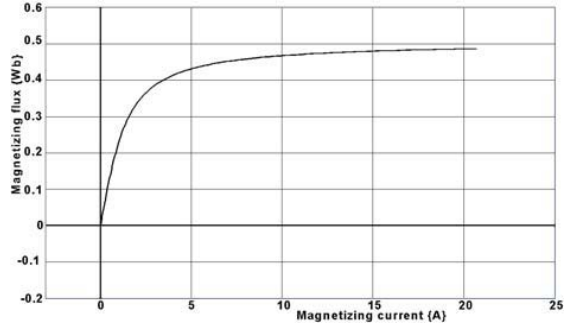


Fig. 4. Saturation curve of equation (49).

In other wise the magnetization inductance of the transformer is defined by

$$L_m = \frac{d\lambda_m}{di_m} = \frac{\alpha\beta}{1 + \beta^2 i_m^2} \quad (50)$$

and substituting into (48) we have

$$\dot{z} = \check{A}z + \overline{B}_p u + G\gamma(Hz) \quad (51)$$

where

$$\check{A} = \begin{bmatrix} \frac{-(R_1+R_m)}{aL_{l2}} & \frac{-R_m}{aL_{l1}} & \frac{R_m}{L_{l1}} \\ \frac{-R_m}{aL_{l2}} & \frac{-(R_2+R_m/a^2)}{aL_{l2}} & \frac{R_m}{L_{l1}} \\ \frac{R_m}{\alpha\beta} & \frac{R_m}{\alpha\beta a} & \frac{-R_m}{\alpha\beta} \end{bmatrix} \quad (52)$$

$$G\gamma(Hz) = \frac{\beta R_m}{\alpha} \left( z_1 z_3^2 + \frac{1}{a} z_2 z_3^2 - z_3^3 \right) \quad (53)$$

also

$$G = \begin{bmatrix} 0 & 0 & \frac{\beta R_m}{\alpha} \end{bmatrix}^T \quad (54)$$

$$\gamma(v) = z_1 z_3^2 + \frac{1}{a} z_2 z_3^2 - z_3^3 \quad (55)$$

and

$$v = Hz = \begin{bmatrix} 1 & \frac{1}{a} & -1 \end{bmatrix} \begin{bmatrix} z_1 \\ z_2 \\ z_3 \end{bmatrix} \quad (56)$$

therefore

$$\frac{\partial \gamma}{\partial v} + \left( \frac{\partial \gamma}{\partial v} \right)^T = 2z_3^2 \geq 0 \quad \forall v \in \mathfrak{R} \quad (57)$$

The numerical values of the parameters of the bond graph of Fig. 3 are  $L_{l1} = 11.05mH$ ,  $L_{l2} = 11.05mH$ ,  $\alpha = 0.3215$ ;  $\beta = 0.8642$ ;  $R_1 = 5.8\Omega$ ,  $R_2 = 5.8\Omega$ ,  $R_L = 100\Omega$ ,  $a = 10$ ,  $R_m = 4K\Omega$  and  $v_1 = 120 \sin(377t)$  and considering a linear performance of the core, the Fig. 4 shows the simulation of this transformer.

If we introduce (49) to the bond graph model of Fig. 3, the nonlinear phenomena is incorporated. Fig. 5 shows the saturation performance in the bond graph model of the transformer.



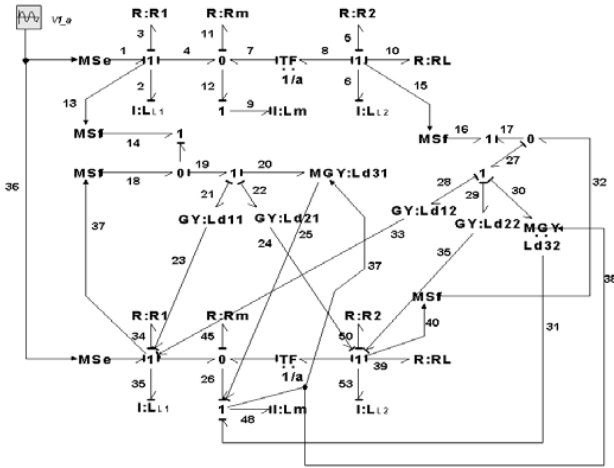


Fig. 9. Observer for the transformer in the physical domain.

The nonlinear section for the observer on the bond graph by using modulated gyrators  $MGY:Ld_{31}$  and  $MGY:Ld_{32}$  with active bonds 37 and 38 is introduced.

In order to prove that the complete bond graph of Fig. 9 represents a system with multivariable monotone nonlinearities, the mathematical model is obtained. Thus, the key vectors for the transformer is given by (44) and for the observer are,

$$\hat{x} = \begin{bmatrix} p_{35} \\ p_{53} \\ p_{48} \end{bmatrix}; \dot{\hat{x}} = \begin{bmatrix} e_{35} \\ e_{53} \\ e_{48} \end{bmatrix}; \hat{z} = \begin{bmatrix} f_{35} \\ f_{53} \\ f_{48} \end{bmatrix}$$

$$\hat{D}_{in} = \begin{bmatrix} f_{34} \\ f_{50} \\ f_{45} \\ f_{39} \end{bmatrix}; \hat{D}_{out} = \begin{bmatrix} e_{34} \\ e_{50} \\ e_{45} \\ e_{39} \end{bmatrix}; y = \begin{bmatrix} f_2 \\ f_6 \\ f_{35} \\ f_{53} \end{bmatrix} \quad (65)$$

the constitutive relations of the elements are,

$$F = \text{diag} \left\{ \frac{1}{L_{11}}, \frac{1}{L_{11}}, \frac{1}{L_m} \right\} \quad (66)$$

$$L = \text{diag} \{ R_1, R_2, R_m, R_L \} \quad (67)$$

and the junction structure is,

$$\hat{S}_{11} = \begin{bmatrix} Ld_{11} & Ld_{12} & 0 \\ Ld_{21} & Ld_{22} & 0 \\ Ld_{31} & Ld_{32} & 0 \end{bmatrix}; \hat{S}_{13} = \begin{bmatrix} 1 & 0 \\ 0 & 1 \\ 0 & 0 \end{bmatrix}$$

$$\hat{S}_{12} = \begin{bmatrix} -1 & 0 & -1 & 0 \\ 0 & -1 & -a^{-1} & -1 \\ 0 & 0 & 1 & 0 \end{bmatrix}; \hat{S}_{31} = \begin{bmatrix} 1 & 0 & 0 \\ 0 & 1 & 0 \end{bmatrix}$$

$$\hat{S}_{22} = \hat{S}_{23} = \hat{S}_{32} = \hat{S}_{33} = 0 \quad (68)$$

From (61), (62), (66), (67) and (68) the state space representation is,

$$\hat{A}_p = \begin{bmatrix} \frac{-R_{11}}{L_{11}} + G_{11} & \frac{-a^{-1}R_m}{L_{11}} + G_{12} & \frac{R_m}{L_{11}} \\ \frac{-a^{-1}R_m}{L_{12}} + G_{21} & \frac{-R_{22}}{L_{12}} + G_{22} & \frac{-a^{-1}R_m}{L_{12}} \\ \frac{R_m}{L_m} + \frac{Lp_{31}}{L_m} & \frac{-a^{-1}R_m}{L_m} + \frac{Lp_{32}}{L_m} & \frac{-R_m}{L_m} \end{bmatrix}$$

$$B_p = \begin{bmatrix} 1 & 0 \\ 0 & 1 \\ 0 & 0 \end{bmatrix}; \tilde{A}_p = \begin{bmatrix} -G_{11} & -G_{12} & 0 \\ -G_{21} & -G_{22} & 0 \\ \frac{-Lp_{31}}{L_m} & \frac{-Lp_{32}}{L_m} & 0 \end{bmatrix} \quad (69)$$

where  $R_{11} = R_1 + R_m$ ;  $R_{22} = R_2 + R_L + R_m$ ;  $G_{11} = Ld_{11}/L_{11}$ ;  $G_{12} = Ld_{12}/L_{11}$ ;  $G_{21} = Ld_{21}/L_{12}$ ;  $G_{22} = Ld_{22}/L_{12}$ ;  $Lp_{31} = (Ld_{31} + K_{d1}L_m)$ ;  $Lp_{32} = (Ld_{32} + K_{d2}L_m)$

$$Lp_{31} = (Ld_{31} + K_{d1}L_m)$$

$$Lp_{32} = (Ld_{32} + K_{d2}L_m)$$

In order to verify that (69) is the same observer respect (51). By substituting (50) into the third line of  $\hat{A}_p$  from (69) we have,

$$\dot{\hat{z}}_3 = \frac{R_m}{\alpha\beta} (\hat{z}_1 + a^{-1}\hat{z}_2 - \hat{z}_3) + \frac{\beta R_m}{\alpha} (\hat{z}_1 + a^{-1}\hat{z}_2 - \hat{z}_3) \hat{z}_3^2 + G \quad (70)$$

where

$$G = (Ld_{31} + K_{d1}L_m) \frac{(\hat{z}_1 - z_1)}{L_m} + (Ld_{32} + K_{d2}L_m) \frac{(\hat{z}_2 - z_2)}{L_m} \quad (71)$$

and using one more time (50) into (71) we obtain,

$$G = K_1 (\hat{z}_1 - z_1) + \frac{\beta}{\alpha} Ld_{31} (\hat{z}_1 - z_1) \hat{z}_3^2 + K_2 (\hat{z}_2 - z_2) + \frac{\beta}{\alpha} Ld_{32} (\hat{z}_2 - z_2) \hat{z}_3^2 \quad (72)$$

Finally, from (36) the original observer gains are

$$L = \begin{bmatrix} L_{11} & L_{12} \\ L_{21} & L_{22} \\ L_{31} & L_{32} \end{bmatrix}; K = [ K_1 \quad K_2 ] \quad (73)$$

Therefore, the relations between the graphical gains in bond graph and the original gains for the observer are:  $Ld_{11} = L_{11} \cdot L_{11}$ ;  $Ld_{12} = L_{12} \cdot L_{11}$ ;  $Ld_{21} = L_{21} \cdot L_{12}$ ;  $Ld_{22} = L_{22} \cdot L_{12}$ ;  $Ld_{31} = \frac{\alpha}{\beta} L_{31}$ ;  $Ld_{32} = \frac{\alpha}{\beta} L_{32}$ ;  $K_{d1} = K_1 - \frac{L_{31}}{\beta^2}$  and  $K_{d2} = K_2 - \frac{L_{32}}{\beta^2}$ .

By substituting the values of the parameters of the complete system according with (35), we have,

$$A = \begin{bmatrix} -362515.83 & -3619909.502 & 361990.9502 \\ -3619909.502 & -36208669.68 & 3619909.502 \\ 14396.7595 & 143967.595 & -14396.7595 \end{bmatrix}$$

$$B = \begin{bmatrix} 90.49 & 0 \\ 0 & 0 \\ 0 & 0 \end{bmatrix}; C = \begin{bmatrix} 1 & 0 & 0 \\ 0 & 1 & 0 \end{bmatrix}$$

$$H = [ 1 \quad 0.1 \quad -1 ]; G = [ 0 \quad 0 \quad 10752.09 ]^T$$

The linear matrix inequality LMI must be feasible (43), which guarantees a strict positive real (SPR) property for the linear part of the observer error system, for this system, we obtain

$$P = \begin{bmatrix} 404427 & -404427 & -0.000566 \\ -404427 & 404427.1 & -0.000836 \\ -0.000566 & -0.000836 & 0.000093 \end{bmatrix}$$

$$L = \begin{bmatrix} -104334.8 & -1035963.5 \\ -104334.8 & -1035963.5 \\ -2306330.8 & -22903046.7 \end{bmatrix}; K = \begin{bmatrix} 5.09 \\ 0.79 \end{bmatrix}^T$$

with  $v = 100$ .

The performance of the electrical transformer with the transformer is shown in Fig. 10 and 11. Fig. 10 illustrates the

primary current on the transformer,  $f_2$  and on the observer,  $f_{35}$ .

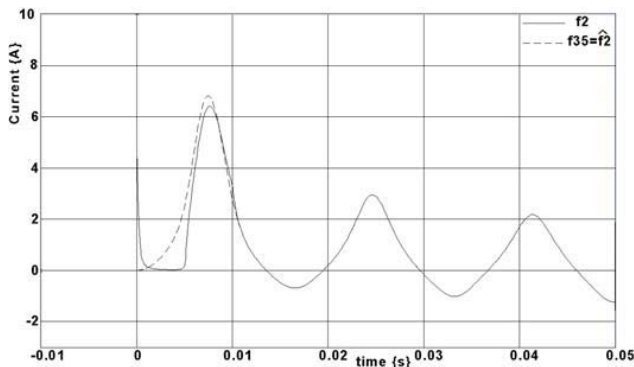


Fig. 10. Primary currents on the transformer and on the observer.

The secondary currents on the transformer,  $f_6$  and on the observer,  $f_{53}$  are shown in Fig. 11.

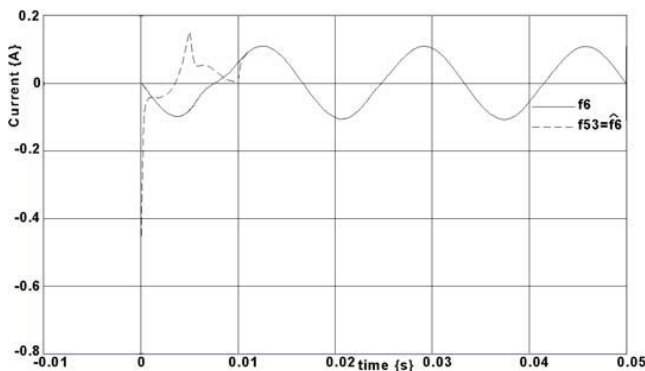


Fig. 11. Secondary currents on the transformer and on the observer.

Therefore, the convergency of the estimates respect the true states of the electrical transformer including nonlinear saturation and hysteresis is guaranteed.

## VIII. CONCLUSIONS

A bond graph model of a power transformer incorporating the nonlinear saturation is presented. In order to prove the results the graphical simulations are shown. A nonlinear observer for the electrical transformer in the physical domain is designed. The convergence of the estimates and the states of the transformer by using simulation is described.

## REFERENCES

- [1] George McPerson and Robert D. Laramore, *An Introduction to Electrical Machines and Transformers*, John, Wiley & Sons, 1990.
- [2] Dean C. Karnopp, Donald L. Margolis and Ronald C. Rosenberg, *System Dynamics Modeling and Simulation of Mechatronic Systems*, Wiley, John & Sons, 2000.
- [3] P. E. Wellstead, *Physical System Modelling*, Academic Press, London, 1979.
- [4] C. Pichardo-Almarza, A. Rahmani, G. Dauphin-Tanguy, M. Delgado, "High gain observers for non-linear systems modelled by bond graphs", *Proc. IMechE Part I: J. Systems and Control Engineering*, 219(2005) pp. 477-497.
- [5] Gilberto Gonzalez-A, R. Galindo, "Direct Control in Bond Graph by State Estimated Feedback for MIMO LTI Estimated", *Proceedings of the 2002 IEEE International Conference on Control Applications*, Scotland, pp. 1183-1188.
- [6] Cesar Pichardo-Almarza, A. Rahmani, G. Dauphin-Tanguy, M. Delgado, "Using the Bicausality concept to build reduced order observers in linear invariant systems modelled by bond graph",
- [7] Peter J. Gawthrop, "Physical Model-based Control: A Bond Graph Approach", *Journal of the Franklin Institute*, 332B(3), pp. 285-305, 1995.
- [8] Rafael Martinez-Guerra, J. De Leon-Morales, "On Nonlinear Observers", *Proceedings of the 1997 IEEE International Conference on Control Applications*, pp. 324-328, 1997.
- [9] Xingzhe Fan, M. Arcak, "Observer design for systems with multivariable monotone nonlinearities", *Systems & Control Letters*, 50(2003) pp. 319-330.
- [10] Xingzhe Fan, M. Arcak, "Nonlinear Observer Design for Systems with Multivariable Monotone Nonlinearities", *Proceedings of the 41st IEEE Conference on Decision and Control*, pp. 684-688, 2002.
- [11] Z. Q. Wu, G. H. Shirkoohi, J. Z. Cao, "Simple dynamic hysteresis modelling of three phase power transformer", *Journal of Magnetism and Magnetic Materials* 160(1996) pp.79-80.
- [12] Chee-Mun Ong, *Dynamic Simulation of Electric Machinery Using MatLab/Simulink*, Prentice-Hall, 1998.
- [13] H. Fraise, J. P. Masson, F. Marthouret and H. Morel, "Modeling od a Non-Linear Conductive Magnetic Circuit. Part 2: Bond Graph Formulation", *IEEE Transactions on Magnetics* Vol. 31, No. 6, November 1995.
- [14] C. Sueur and G. Dauphin-Tanguy, "Bond graph approach for structural analysis of MIMO linear systems", *Journal of the Franklin Institute*, Vol. 328, No. 1, pp. 55-70, 1991.
- [15] S. Garcia, A. Medina and C. Perez, "A state space single-phase transformer model incorporating nonlinear phenomena of magnetic saturation and hysteresis for transient and period steady-state analysis", *IEEE Power Engineering Society Summer Meeting*, Vol. 4, pp. 2417-2421, July 2000.
- [16] M. Arcak, P. Kokotovic, Nonlinear observers: a circle criterion design and robustness, *Automatica* 37(12) (2001) 1923-1930.